# Enhanced acceleration of energetic ions by oblique shock waves

Tomohiro Masaki, Hiroki Hasegawa, and Yukiharu Ohsawa
*Department of Physics, Nagoya University, Nagoya 464-8602, Japan*

(Received 25 June 1999; accepted 19 October 1999)

Interactions of energetic ions with a shock wave propagating obliquely to a magnetic field are studied by means of a one-dimensional, relativistic, electromagnetic, particle simulation code with full ion and electron dynamics. It is found that energetic ions that barely enter the shock region can be accelerated by the transverse electric field. At the same time, their parallel momenta are increased by the magnetic field. Because of this, after the encounter with the shock wave, some of the energetic ions can move with it for long periods of time during which they undergo the acceleration repeatedly. These particles eventually go away from the shock wave to the upstream region, and their acceleration ceases. © *2000 American Institute of Physics.* [S1070-664X(00)01402-6]

## I. INTRODUCTION

It has been known that extremely high-energy particles are produced in astrophysical plasmas[1–4] and in laboratory plasmas.[5] Motivated by these observations and experiments, many theoretical and computational studies have been made.[6–25] In particular, particle simulations have demonstrated that magnetosonic shock waves can produce high-energy ions[8–16] and electrons.[17,18] (There are, of course, various acceleration models which do not use shock waves; see, for instance, Ref. 6.) From these simulations, we now know several different mechanisms of particle acceleration in shock waves. For instance, in a single-ion-species plasma, the electric potential formed in a shock wave can reflect some of the ions and give great energies to them,[8–14,19–22] In a multi-ion-species plasma, like space plasmas, the same mechanism operates on hydrogen ions, which are the main components of ions. Minor heavy ions such as He, C, and Fe are all accelerated to nearly the same speed by the transverse electric field.[15,16] On the other hand, ultrarelativistic electrons can be produced by the strong electric field parallel to the magnetic field;[17,18] this can take place in an oblique shock wave in a rather strong magnetic field. These are the mechanisms accelerating particles from thermal-level energies to much higher, nonthermal energies.

In those studies, interactions of particles with one shock wave (or large-amplitude pulse) were considered. In a plasma with strong magnetohydrodynamic turbulence, however, particles would successively encounter many different magnetosonic shock waves. Such multiple collisions with pulses will occur, for instance, in solar flares. Also, particles around a pulsar may repeatedly encounter large-amplitude pulses going away from the pulsar. (A large-amplitude pulse will quickly steepen into a quasi-shock wave. Hence we will also call it a shock wave.)

After the passage of a shock wave, there would be some energetic particles left because of the processes mentioned above (or by some other mechanisms). These energetic particles will also successively collide with other different shock waves. Now, if shock waves have any mechanisms that can further accelerate energetic particles, we will have extremely high-energy particles in plasmas with strong magnetohydrodynamic turbulence or in plasmas around pulsars. It is thus quite important to study how energetic particles interact with magnetosonic shock waves.

To account for the anomalous cosmic rays,[23] Lee *et al.*[21] proposed an acceleration model for pickup ions. This is also a kind of interaction between high-energy ions and shock waves, even though the mechanism is completely different from the one discussed in this paper.

Maruyama *et al.*[24] numerically and theoretically studied the interaction between energetic ions and a magnetosonic shock wave. They considered a perpendicular shock wave in a plasma consisting of electrons, bulk thermal ions, and a small number of nonthermal energetic ions. Speeds of the energetic ions were supposed to be much higher than the shock propagation speed. Hence, the ions that barely enter the shock region can go out to the upstream region (at least) once, even though they eventually move to the downstream region for a perpendicular shock wave. The particle simulations showed that those energetic ions can be further accelerated to higher energies. The acceleration occurs because, when they are in the shock region, their gyromotions are nearly parallel to the transverse electric field formed in the shock wave. The amount of energy that an energetic ion can gain in this way was theoretically obtained. The theory and simulations both showed that the ions having higher energies can gain greater energies. These results suggest that in a plasma with strong magnetohydrodynamic turbulence some of the ions could be repeatedly accelerated to higher energies by the collisions with many different shock waves.

The above work was for perpendicular shock waves. Thus, particle momentum parallel to the magnetic field was a constant of motion. In a shock wave propagating obliquely to a magnetic field, however, parallel momentum of a particle can change with time. Moreover, some particles can move with a shock wave for long periods of time because of the motion along the field lines. Hence, some new phenomena may appear in oblique shock waves.

In this paper we will study the interaction of energetic ions with an oblique shock wave, giving special attention to effects of particle motion along the field line. (Preliminary results have been reported in Ref. 25.)

In Sec. II, we theoretically discuss the motion of ener-

 

getic ions in an oblique shock wave. As in the previous paper,[24] we mainly consider a particle that barely enters the shock region, which quickly goes out to the upstream region at least once. Then, we will find that its momentum parallel to the magnetic field, $p_\parallel$, increases owing to the change in the direction of the magnetic field $\boldsymbol{B}$; in a one-dimensional oblique shock wave the magnetic field parallel to the wave front is strong in the shock region while the magnetic field in the direction of the wave normal is constant, and thus the direction of $\boldsymbol{B}$ is changed. This increase in the parallel momentum occurs twice; just when the particle enters and goes out of the shock region. This process does not change the particle energy. However, while the particle is in the shock region, the transverse electric field can increase the kinetic energy by the same mechanism as the one discussed in Ref. 24.

Now suppose that the shock wave is propagating in the $x$ direction with speed $v_{\rm sh}$, and let $v_\parallel$ be the parallel speed of a particle and $v_{\parallel x}$ be the $x$ component of the parallel velocity. Then, even if the initial $v_\parallel$ is small (and thus $v_{\parallel x}$ is smaller than $v_{\rm sh}$), the collision with the shock wave can make $v_{\parallel x}$ closer to the shock speed $v_{\rm sh}$; because it can increase $p_\parallel$. Of the ions with initial $v_{\parallel x}$ smaller than $v_{\rm sh}$, therefore, some can move with the shock wave for long periods of time.

In Sec. III, we study the evolution of a shock wave and motions of electrons, thermal ions, and energetic ions in a self-consistent manner by using a one-dimensional (one space coordinate and three velocity components), relativistic, electromagnetic, particle simulation code with full ion and electron dynamics. The theoretical prediction mentioned above will be confirmed. Furthermore, it will be found that some energetic ions can be accelerated several times by the transverse electric field in a shock wave; the acceleration mechanism can operate repeatedly on some particles. These are the particles that move with the shock wave for long periods of time. During these periods, $p_\parallel$, as well as the kinetic energy of each particle is increased, and $v_{\parallel x}$ finally exceeds $v_{\rm sh}$. Then, these particles go ahead of the shock wave, and the interactions with the wave cease. This is also an important feature of this phenomenon; in the acceleration mechanisms mentioned above,[8–24] energized particles eventually move to the downstream region.

In Sec. IV, we will summarize our work and will discuss the condition that the multiple acceleration can take place.

## II. MOTION OF ENERGETIC IONS

We consider energetic ions whose speeds are much higher than shock propagation speed $v_{\rm sh}$. If they barely enter the shock region, they would quickly go out again to the upstream region. Figure 1 shows such an orbit in a perpendicular shock wave. Here, an energetic ion enters the shock region at $t=t_{\rm in}$ and goes out at $t=t_{\rm out}$; the solid and dotted vertical lines represent the positions of the wave front at $t=t_{\rm in}$ and $t=t_{\rm out}$, respectively, and $\rho$ is the gyro-radius in the shock region. As can be seen from Fig. 1, when the particle is in the shock region, its velocity is always nearly parallel to the transverse electric field of the shock wave. In Ref. 24,

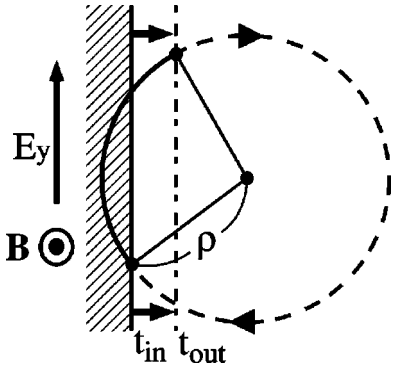


FIG. 1. Orbit of an energetic ion that barely enters the shock region.

perpendicular shock waves were considered. In this section we will analytically discuss motions of energetic ions in an oblique shock wave.

### A. Effect of magnetic field

First, we will show that the change in the direction of the magnetic field can lead to the increase in the momentum of an energetic ion parallel to the magnetic field, $p_\parallel$. We assume that a shock wave is propagating in the $x$ direction ($\partial/\partial y=\partial/\partial z=0$) in an external magnetic field in the $(x,z)$ plane. We consider a particle which enters the shock region at time $t=t_{\rm in}$ and, after a short while, goes out again to the upstream region at time $t=t_{\rm out}$ (see Fig. 2). The gyro-radius of an energetic ion is much larger than the scale length of the shock ramp, where plasma density, potential, and magnetic field rapidly rise. Therefore, the time rate of change of the magnetic field that an energetic ion feels along its orbit can be expressed as

$$\frac{d\boldsymbol{B}}{dt}=(\boldsymbol{B}_1-\boldsymbol{B}_0)[\,\delta(t-t_{\rm in})-\delta(t-t_{\rm out})\,]. \tag{1}$$

Here, the subscripts 0 and 1 refer to the quantities measured in the upstream and shock regions, respectively. Both $\boldsymbol{B}_0$ and

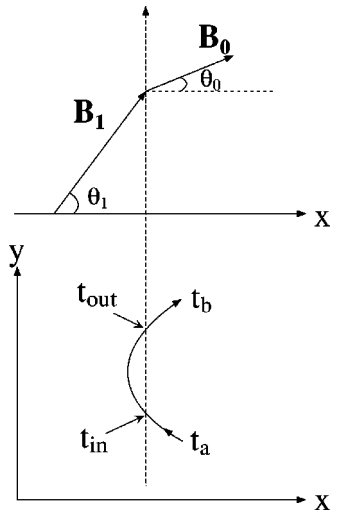


FIG. 2. Schematic diagram of magnetic field and ion orbit. Here $B_0$ and $B_1$ represent magnetic fields in the upstream and shock regions, respectively.

$\boldsymbol{B}_1$ are assumed to be constant. For the definiteness, we assume that $B_{0x}>0$ and $B_{0z}>0$. Then, $B_{1z}$ would be positive and greater than $B_{0z}$. The $x$ component is constant, $B_{1x}=B_{0x}$, because $\partial/\partial y=\partial/\partial z=0$. The $y$ component can have finite values in the shock region. However, we neglect $B_{1y}$ in this section, because it is nearly zero at the location where $B_{1z}$ is large; for the shock structure, see Refs. 18, 26–31.

In this subsection, we focus on the effect of the change in the magnetic field. Hence, we consider particle motion in the absence of electric fields. It follows from the equation of motion,

$$\frac{d\boldsymbol{p}}{dt}=q\left(\boldsymbol{E}+\frac{\boldsymbol{v}}{c}\times\boldsymbol{B}\right), \tag{2}$$

that

$$\frac{d\boldsymbol{p}}{dt}\cdot\boldsymbol{B}=0, \tag{3}$$

for $\boldsymbol{E}=0$. We thus have

$$\frac{d(\boldsymbol{p}\cdot\boldsymbol{B})}{dt}=\boldsymbol{p}\cdot\frac{d\boldsymbol{B}}{dt}. \tag{4}$$

Substituting Eq. (1) in Eq. (4) and integrating over time from $t=t_a$ (the time right before $t=t_{\rm in}$) to $t=t_b$ (the time right after $t=t_{\rm out}$), we find

$$\boldsymbol{p}(t_b)\cdot\boldsymbol{B}(t_b)-\boldsymbol{p}(t_a)\cdot\boldsymbol{B}(t_a)=[\boldsymbol{p}(t_{\rm in})-\boldsymbol{p}(t_{\rm out})]\cdot(\boldsymbol{B}_1-\boldsymbol{B}_0). \tag{5}$$

At $t=t_a$ and $t=t_b$, the particle is in front of the shock wave; therefore, $\boldsymbol{B}(t_a)=\boldsymbol{B}(t_b)=\boldsymbol{B}_0$. The left-hand side of Eq. (5) is thus equal to $[\boldsymbol{p}_0(t_b)-\boldsymbol{p}_0(t_a)]\cdot\boldsymbol{B}_0$, where only the parallel component of $\boldsymbol{p}_0$ contributes. Let $\delta p_\parallel$ be the increase in the momentum parallel to $\boldsymbol{B}_0$,

$$\delta p_\parallel=[\boldsymbol{p}_0(t_b)-\boldsymbol{p}_0(t_a)]\cdot\boldsymbol{B}_0/B_0, \tag{6}$$

then the left-hand side of Eq. (5) is equal to $\delta p_\parallel B_0$.

Because of the change in the direction of the magnetic field, the magnitudes of the parallel and perpendicular components of the momentum change when an energetic particle enters the shock region. It is also the case when it goes out again to the upstream region. That is, even though the momentum is continuous, $\boldsymbol{p}(t_{\rm in})=\boldsymbol{p}_0(t_{\rm in})=\boldsymbol{p}_1(t_{\rm in})$, $p_{1\parallel}(t_{\rm in})$ is not equal to $p_{0\parallel}(t_{\rm in})$, because $\boldsymbol{B}_1$ is not parallel to $\boldsymbol{B}_0$. In Fig. 3, we show $\boldsymbol{B}_0$, $\boldsymbol{B}_1$, and $\boldsymbol{p}$ at $t=t_{\rm in}$ (upper panel) and $t=t_{\rm out}$ (lower panel); note that $\boldsymbol{p}_{1\parallel}+\boldsymbol{p}_{1\perp}=\boldsymbol{p}_{0\parallel}+\boldsymbol{p}_{0\perp}$ in either case. Furthermore, because $\boldsymbol{E}$ is neglected here, $p_{1\parallel}(t)$ is constant during the time from $t=t_{\rm in}$ to $t=t_{\rm out}$. We therefore have

$$\boldsymbol{p}(t_{\rm in})-\boldsymbol{p}(t_{\rm out})=\boldsymbol{p}_{1\perp}(t_{\rm in})-\boldsymbol{p}_{1\perp}(t_{\rm out}). \tag{7}$$

Then, noting that $\boldsymbol{p}_{1\perp}\cdot\boldsymbol{B}_1=0$, we have

$$[\boldsymbol{p}(t_{\rm in})-\boldsymbol{p}(t_{\rm out})]\cdot(\boldsymbol{B}_1-\boldsymbol{B}_0)=[\boldsymbol{p}_{1\perp}(t_{\rm out})-\boldsymbol{p}_{1\perp}(t_{\rm in})]\cdot\boldsymbol{B}_0. \tag{8}$$

Equation (5) thus gives the increase in the parallel momentum as

$$\delta p_\parallel=[\boldsymbol{p}_{1\perp}(t_{\rm out})-\boldsymbol{p}_{1\perp}(t_{\rm in})]\cdot\boldsymbol{B}_0/B_0. \tag{9}$$

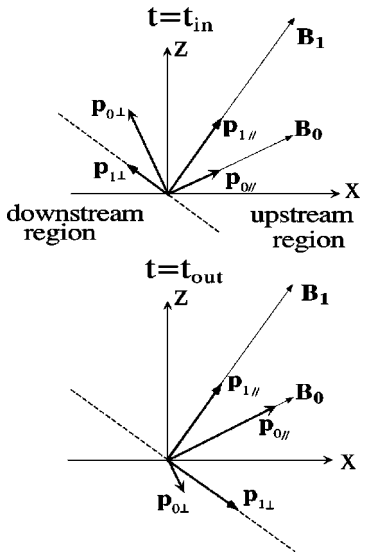


FIG. 3. Schematic diagram of magnetic fields and momenta at $t=t_{\rm in}$ and at $t=t_{\rm out}$. They are projected on the $(x,z)$ plane.

As one moves from the upstream region to the shock region, the $z$ component of the magnetic field, $B_z$, greatly increases, while $B_x$ is constant in time and space.[18,30,31] Hence, the inner product $\boldsymbol{p}_{1\perp}(t_{\rm in})\cdot\boldsymbol{B}_0$ is always negative. Indeed, because $p_{1\perp x}(t_{\rm in})<0$ and hence $p_{1\perp z}(t_{\rm in})>0$, the right-hand side of the following equation:

$$\boldsymbol{p}_{1\perp}(t_{\rm in})\cdot\boldsymbol{B}_1-\boldsymbol{p}_{1\perp}(t_{\rm in})\cdot\boldsymbol{B}_0=p_{1\perp z}(B_{1z}-B_{0z}), \tag{10}$$

is positive, while the first term on the left-hand side is zero. Hence, $\boldsymbol{p}_{1\perp}(t_{\rm in})\cdot\boldsymbol{B}_0<0$. In the same way we see that $\boldsymbol{p}_{1\perp}(t_{\rm out})\cdot\boldsymbol{B}_0$ is always positive. One can see this also from Fig. 3.

The right-hand side of Eq. (9) is thus always positive. That is, if an energetic ion enters the shock region and goes out again to the upstream region, its parallel momentum increases, $\delta p_\parallel>0$. This is caused by the magnetic field; hence the magnitude of the momentum does not change. In this process, perpendicular momentum decreases.

The $x$ component of the parallel velocity, $v_{\parallel x}$, may be given by $v_\parallel\cos\theta$, where $\theta$ is the angle between the magnetic field and the $x$ axis. The above result suggests that $v_\parallel$ can increase by the interaction with the shock wave. Therefore, even if $v_{\parallel x}$ is initially lower than the shock speed $v_{\rm sh}$, it can become close to $v_{\rm sh}$, $v_\parallel\cos\theta\sim v_{\rm sh}$, after the collision with the shock wave. Such a particle will be able to move with the shock wave for a long time.

### B. Energy gain from electric field

It was shown in Ref. 24 that some of the energetic ions can obtain great energies from the transverse electric field in a perpendicular shock wave. We now examine this acceleration mechanism for oblique shock waves, including effects of electric fields. As in the previous subsection, the fields are assumed to be constant in the shock and upstream regions; the changes occur at the boundary of these regions.

The unperturbed orbit in a constant magnetic field,

$$\boldsymbol{B}=B(\cos\theta,0,\sin\theta), \tag{11}$$

can be described as

$$x(t)=v_{\parallel}t\cos\theta+\rho\sin\theta\cos(-\omega_{ci}t+\eta)+x_0, \tag{12}$$

$$y(t)=\rho\sin(-\omega_{ci}t+\eta)+y_0, \tag{13}$$

$$z(t)=v_{\parallel}t\sin\theta-\rho\cos\theta\cos(-\omega_{ci}t+\eta)+z_0, \tag{14}$$

where $\rho$ is the gyro-radius, $\eta$ is the initial phase, and $x_0$, $y_0$, and $z_0$ are constant; $\omega_{ci}$ is the ion cyclotron frequency,

$$\omega_{ci}=q_iB/(m_ic\gamma), \tag{15}$$

with $\gamma$ the Lorentz factor. The momentum is given as

$$p_x(t)=p_{\parallel}\cos\theta+p_{\perp}\sin\theta\sin(-\omega_{ci}t+\eta), \tag{16}$$

$$p_y(t)=-p_{\perp}\cos(-\omega_{ci}t+\eta), \tag{17}$$

$$p_z(t)=p_{\parallel}\sin\theta-p_{\perp}\cos\theta\sin(-\omega_{ci}t+\eta). \tag{18}$$

Taking the scalar product of the equation of motion, (2), with $\boldsymbol{p}$, we have

$$\frac{d}{dt}\left(\frac{p^2}{2}\right)=q\boldsymbol{p}\cdot\boldsymbol{E}. \tag{19}$$

We consider the motion in the shock region. If we integrate Eq. (19) over time from $t=t_{\rm in}$ to $t=t_{\rm out}$, we obtain the increase in $p^2$ as

$$\delta\left(\frac{p^2}{2}\right)=q\int_{t_{\rm in}}^{t_{\rm out}}(p_xE_x+p_yE_y+p_zE_z)dt. \tag{20}$$

Substituting the unperturbed orbit, Eqs. (12)–(18), in the terms on the right-hand side, we have

$$\begin{aligned}\delta\left(\frac{p^2}{2}\right)=q\int_{t_{\rm in}}^{t_{\rm out}}&[p_{\parallel}(E_x\cos\theta+E_z\sin\theta)\\&+p_{\perp}(E_x\sin\theta-E_z\cos\theta)\sin(-\omega_{ci}t+\eta)\\&-p_{\perp}E_y\cos(-\omega_{ci}t+\eta)]dt.\end{aligned} \tag{21}$$

We note that $E_{\parallel}=E_x\cos\theta+E_z\sin\theta$. Also, because we use the unperturbed orbit, $p_{\parallel}$ and $p_{\perp}$, on the right-hand side are constant. Consequently, we find

$$\begin{aligned}\delta\left(\frac{p^2}{2}\right)=&qp_{1\parallel}E_{\parallel}(t_{\rm out}-t_{\rm in})-\frac{2qp_{1\perp}}{\omega_{ci}}(E_x\sin\theta-E_z\cos\theta)\\&\times\sin\left(-\frac{\omega_{ci}(t_{\rm out}+t_{\rm in})}{2}+\eta\right)\sin\left(-\frac{\omega_{ci}(t_{\rm out}-t_{\rm in})}{2}\right)\\&+\frac{2qp_{1\perp}}{\omega_{ci}}E_y\cos\left(-\frac{\omega_{ci}(t_{\rm out}+t_{\rm in})}{2}+\eta\right)\\&\times\sin\left(-\frac{\omega_{ci}(t_{\rm out}-t_{\rm in})}{2}\right).\end{aligned} \tag{22}$$

We focus on the particles that are in the shock region for short time periods,

$$\omega_{ci}(t_{\rm out}-t_{\rm in})\ll 1; \tag{23}$$

thus we can assume that

$$\cos\left(-\frac{\omega_{ci}(t_{\rm out}+t_{\rm in})}{2}+\eta\right)\simeq-1. \tag{24}$$

Then, Eq. (22) gives

$$\begin{aligned}\delta\left(\frac{p^2}{2}\right)=&qp_{1\parallel}E_{\parallel}(t_{\rm out}-t_{\rm in})\\&-\frac{2qp_{1\perp}}{\omega_{ci}}E_y\sin\left(-\frac{\omega_{ci}(t_{\rm out}-t_{\rm in})}{2}\right).\end{aligned} \tag{25}$$

Because of the inequality (23), this equation can be further simplified as

$$\delta\left(\frac{p^2}{2}\right)\simeq q(p_{1\parallel}E_{\parallel}+p_{1\perp}E_y)(t_{\rm out}-t_{\rm in}). \tag{26}$$

We now estimate the time period $(t_{\rm out}-t_{\rm in})$. In this period the shock wave traverses a length $v_{\rm sh}(t_{\rm out}-t_{\rm in})$. This is equal to the change in the $x$ position of the particle, $x(t_{\rm out})-x(t_{\rm in})$. Hence, with the aid of Eq. (12), we have

$$\begin{aligned}&(v_{\rm sh}-v_{\parallel}\cos\theta)(t_{\rm out}-t_{\rm in})\\&\quad=\rho\sin\theta[\cos(-\omega_{ci}t_{\rm out}+\eta)-\cos(-\omega_{ci}t_{\rm in}+\eta)].\end{aligned} \tag{27}$$

We define quantity $d$ as

$$d=-\rho\cos(-\omega_{ci}t_{\rm in}+\eta)(>0). \tag{28}$$

Then, using the relation $\cos(-\omega_{ci}t_{\rm out}+\eta)=\cos[-\omega_{ci}(t_{\rm out}-t_{\rm in})-\omega_{ci}t_{\rm in}+\eta]$, we find that

$$\begin{aligned}\cos(-\omega_{ci}t_{\rm out}+\eta)=&-(d/\rho)\cos[-\omega_{ci}(t_{\rm out}-t_{\rm in})]\\&+(1-d^2/\rho^2)^{1/2}\sin[-\omega_{ci}(t_{\rm out}-t_{\rm in})].\end{aligned} \tag{29}$$

Here, we used the fact that $\sin(-\omega_{ci}t_{\rm in}+\eta)$ is negative. Substituting Eqs. (28) and (29) in Eq. (27), we find the time period as

$$\omega_{ci}(t_{\rm out}-t_{\rm in})\simeq\frac{2(\rho^2-d^2)^{1/2}}{d}+\frac{2(v_{\rm sh}-v_{1\parallel}\cos\theta)}{d\omega_{ci}\sin\theta}, \tag{30}$$

for energetic particles barely entering the shock wave, i.e., for particles satisfying inequality (23). The quantities $\omega_{ci}$, $\rho$, and $\theta$ in this equation should be the ones in the shock region. From Eqs. (26) and (30), we have

$$\begin{aligned}\delta\left(\frac{p^2}{2}\right)\simeq&\frac{2q}{\omega_{ci}d}(p_{1\parallel}E_{\parallel}+p_{1\perp}E_y)\\&\times\left((\rho^2-d^2)^{1/2}+\frac{(v_{\rm sh}-v_{1\parallel}\cos\theta)}{\omega_{ci}\sin\theta}\right).\end{aligned} \tag{31}$$

In magnetohydrodynamic waves, parallel electric fields are usually much weaker than perpendicular ones; later, it will be confirmed by simulations that this is also the case in shock waves. In Eq. (31), therefore, the term $p_{1\perp}E_y$ will predominate over $p_{1\parallel}E_{\parallel}$. This expression for the increase in $p^2$ in an oblique shock wave is quite similar to the one in a perpendicular shock wave. Indeed, when $\theta$ is close to $\pi/2$, Eq. (31) is reduced to Eq. (22) in Ref. 24. The increase in energy $\gamma$ is given by

$$\delta\gamma=\delta(p^2/2)/(m_i^2c^2\gamma). \tag{32}$$

## III. SIMULATION

### A. Simulation method and parameters

We now study the enhanced acceleration by oblique shock waves by means of a one-dimensional (one space coordinate and three velocity components), relativistic, electromagnetic, particle simulation code with full ion and electron dynamics.[32]

The total system length is $L_x = 4096\Delta_g$, where $\Delta_g$ is the grid spacing. All lengths and velocities in the simulations were normalized to $\Delta_g$ and $\omega_{pe}\Delta_g$, respectively, where $\omega_{pe}$ is the spatially averaged plasma frequency. We use a bounded plasma model.[11] The plasma is limited to the region $100 < x < 3996$. The particles are specularly reflected at $x = 100$ and at $x = 3996$. The radiation leaving the plasma region is absorbed in the vacuum regions, $0 < x < 100$ and $3996 < x < 4096$. Thus the electromagnetic interactions between the two plasma boundaries through the vacuum regions are made negligibly small.

As space plasmas, the code contains hydrogen (H), helium (He), and electrons. Ions consist of thermal bulk particles and nonthermal energetic ones. We first describe the thermal ions and electrons. In most of the plasma region, i.e., in $300 < x < 3996$, each particle species initially has a uniform density and has a Maxwellian velocity distribution function. In the small region, $100 < x < 280$, the plasma density is four times as high as that in the main region. The plasma density smoothly decreases as $x$ increases from $x = 280$ to $x = 300$. In the high-density region, particles have shifted Maxwellian velocity distribution functions with average velocity $\boldsymbol{v}_{\rm ps}$; $f_j \sim \exp[-(\boldsymbol{v}-\boldsymbol{v}_{\rm ps})^2/(2v_{Tj}^2)]$, where the subscript $j$ refers to particle species. These particles act as a piston. They push the neighboring particles and excite a shock wave. We can change the shock strength by changing the magnitude of $\boldsymbol{v}_{\rm ps}$; the velocity $\boldsymbol{v}_{\rm ps}$ is perpendicular to the external magnetic field so that no particles have extremely large parallel speeds initially. A more detailed description about the simulation code can be found in Ref. 11.

In addition to the thermal bulk ions, we have nonthermal, energetic ions with small abundances; in the present simulations the abundance of the energetic particles was one percent for each ion species. Their initial energies were set to be the same for each run, and the momentum distributions were isotropic.

The simulation parameters are the following: The ion-to-electron mass ratio is $m_{\rm H}/m_e = 50$; the speed of light is $c = 4$; the electron skin depth is $c/\omega_{pe} = 4$; the initial electron and ion thermal velocities are $v_{Te} = 1.04$ and $v_{T\rm H} = v_{T\rm He} = 0.04$, respectively. The frequency ratio $\omega_{ce}/\omega_{pe}$ is 1.5 in the upstream region; thus, the Alfvén speed is $v_{\rm A} = 0.79$. The ratio between the two ion-cyclotron-frequencies is $\omega_{c\rm H}/\omega_{c\rm He} = 2$. The mass–density ratio is $n_{\rm He}m_{\rm He}/(n_{\rm H}m_{\rm H}) = 0.4$. Keeping these two ratios unchanged, we made the mass and charge of He small; we used the technique of fine particles.[33] Thus the total numbers of simulation ions were $N_{\rm H} = N_{\rm He} = 240{,}000$. The number of electrons was $N_e = 288{,}000$. The time step $\Delta t$ was typically $\omega_{pe}\Delta t = 0.05$, so that $\Delta t$ is much smaller than the plasma and cyclotron periods even in the shock region. The external magnetic field is in the $(x,z)$ plane, and waves propagate in the $x$ direction.

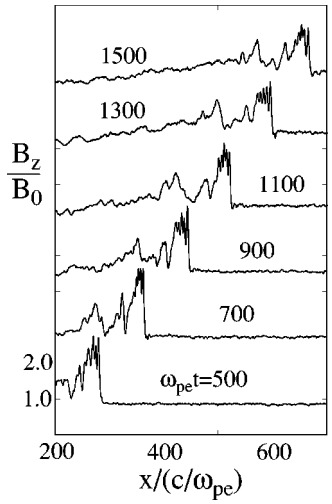


FIG. 4. Profiles of $B_z$ of an oblique shock wave at various times.

### B. Simulation results

We show in Fig. 4 profiles of $B_z$ in an oblique shock wave at various times. Its propagation angle is $\theta = 60°$; i.e.,

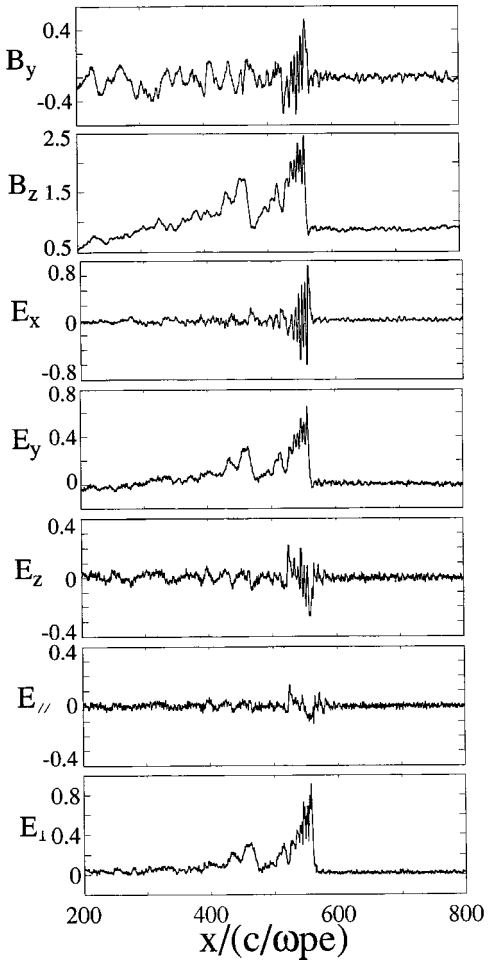


FIG. 5. Snapshots of field profiles. Electric and magnetic field profiles at $\omega_{pe}t = 1200$ are plotted. They are normalized to $B_0$.

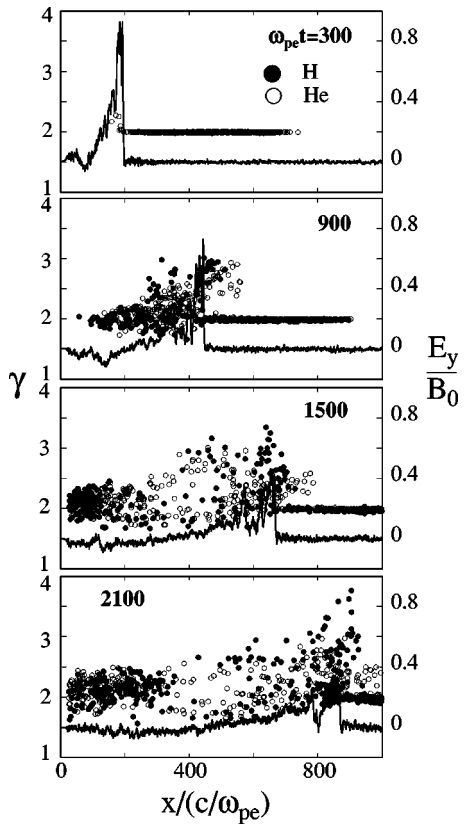


FIG. 6. Phase space plots $(x,\gamma)$ of energetic ions and profiles of $E_y$.

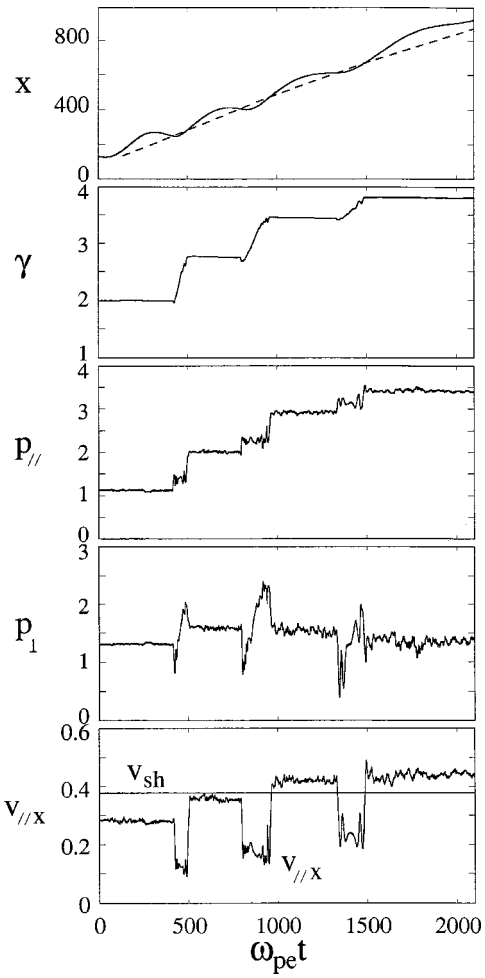


FIG. 7. Time variations of $x$, $\gamma$, $p_\parallel$, $p_\perp$, and $v_{\parallel x}$ of an energetic ion that was further accelerated three times.

$B_{z0}/B_{x0}=\tan 60°$. The shock speed is observed to be $v_{\rm sh}=1.9v_{\rm A}$. Figure 5 displays the field profiles at $\omega_{pe}t=1200$. They are all normalized to the magnetic field strength in the upstream region, $B_0$. In the shock region, $B_z$ is much greater than $B_y$. The electric field $E_y$ has a profile similar to $B_z$. The parallel electric field $E_\parallel$ is much smaller than $E_\perp$; we obtained them from the relations $\boldsymbol{E}_\parallel=(\boldsymbol{B}\cdot\boldsymbol{E})\boldsymbol{B}/B^2$ and $\boldsymbol{E}_\perp=\boldsymbol{E}-\boldsymbol{E}_\parallel$, using the observed data of $\boldsymbol{B}$ and $\boldsymbol{E}$.

We show in Fig. 6 phase space plots $(x,\gamma)$ of energetic ions at various times. The dots and white circles represent H and He, respectively. Their initial values of $\gamma$ were set to be $\gamma=2.0$. Even though the energetic ions were distributed uniformly in space, we show here the particles that were in the region $364\leqslant x/(c/\omega_{pe})\leqslant 533$ at $\omega_{pe}t=0$. The region of these particles is expanding with time by the gyro and parallel motions; the gyro-radius of H ions with $\gamma=2$ is $\rho_{\rm H}/(c/\omega_{pe})=57$ in the upstream region. To observe the interaction with the shock wave, we also plotted, in the same figure, profiles of the transverse electric field $E_y$. The figure indicates that some of the energetic ions are accelerated to higher energies when they encounter the shock wave. By $\omega_{pe}t=2100$, the pulse amplitude has already become small. However, we find especially high-energy particles near the pulse.

We investigate particle motion in more detail. Figure 7 shows time variations of $x$, $\gamma$, $\boldsymbol{p}$, and $v_{\parallel x}$ of an energetic ion that gained a great amount of energy from the shock wave. The top panel shows $x$ positions of the particle (solid line) and the shock front (dotted line); the upstream region is above the dotted line. The particle enters the shock region for the first time at $\omega_{pe}t=410$. When the simulation was finished, i.e., at $\omega_{pe}t=2100$, the particle was in the upstream region, moving slightly faster than the pulse. Its energy $\gamma$ jumped three times. The jump occurs when the particle is in the shock region. The parallel momentum $p_\parallel$ also increases sharply several times. The change in $p_\perp$ is more complex; right before and after the rapid increase, it quickly decreases. The bottom panel shows $v_{\parallel x}$ $(=v_\parallel B_x/B)$. Before the first collision with the shock wave, $v_{\parallel x}$ is smaller than the shock speed $v_{\rm sh}$ (otherwise the shock wave cannot catch up with the particle). After each collision, $v_{\parallel x}$ increases, and finally $v_{\parallel x}$ exceeds $v_{\rm sh}$ and the particle moves away from the shock wave to the upstream region. (In the shock region, $v_{\parallel x}$ is small because $B_z$ is large.) Figure 8 gives expanded views of the second collision in Fig. 7; for the period from $\omega_{pe}t=700$ to $\omega_{pe}t=1050$. Here, the particle enters the shock region at $\omega_{pe}t\simeq 800$ and goes out at $\omega_{pe}t\simeq 960$. At these times, $p_\parallel$ increases and $p_\perp$ decreases. However, during this period, i.e., while the particle is in the shock region, $p_\parallel$ is nearly constant, and $p_\perp$ and $\gamma$ keep increasing. These are in good agreement with the theoretical prediction in Sec. II.

We have seen that some of the energetic ions can be

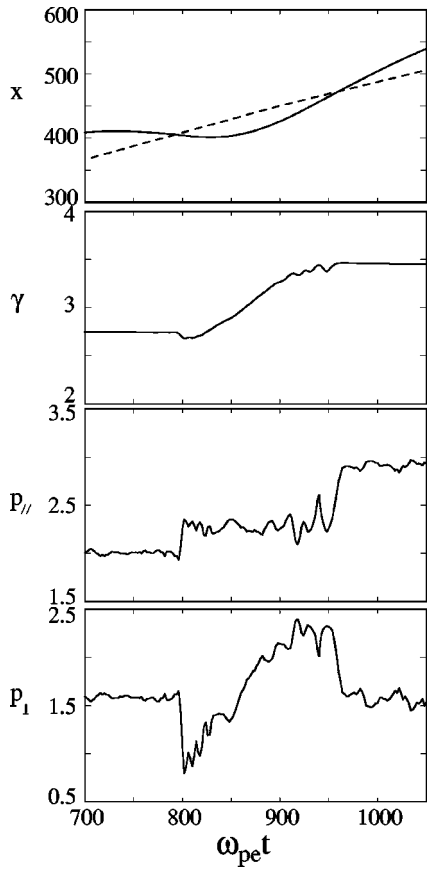


FIG. 8. Expanded views of the time variations of $x$, $\gamma$, $p_\parallel$, $p_\perp$, and $v_{\parallel x}$.

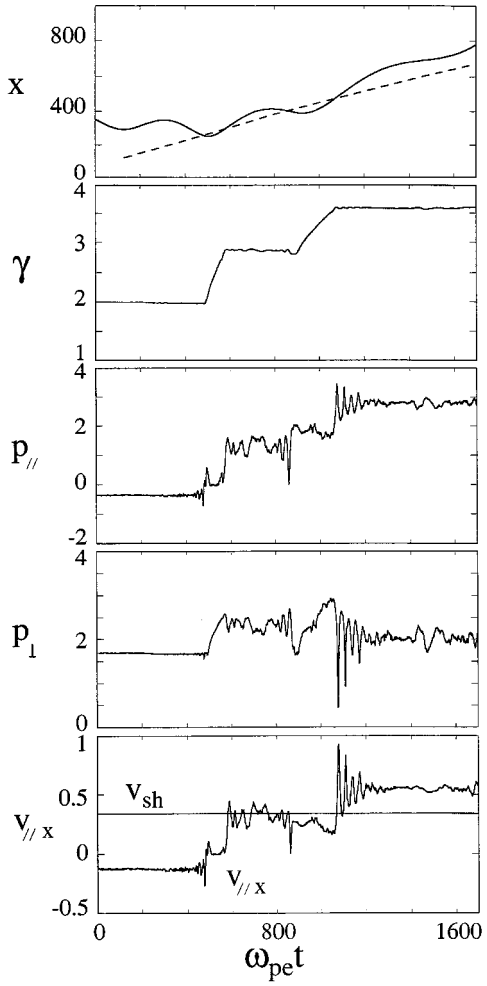


FIG. 9. Time variations of $x$, $\gamma$, $p_\parallel$, $p_\perp$, and $v_{\parallel x}$ of an energetic ion that was further accelerated twice in an oblique shock wave with $\theta=45°$.

accelerated several times by the transverse electric field in an oblique shock wave; the mechanism observed in a perpendicular shock wave[24] can operate several times on one particle. We have also seen that $p_\parallel$ increases ($p_\perp$ decreases) at the moments when the particle enters and goes out of the shock region. We now show some other examples. Figure 9 displays time variations of $x$, $\gamma$, $\boldsymbol{p}$, and $v_{\parallel x}$ of an energetic particle in a shock wave with propagation angle $\theta=45°$. The propagation speed is $v_{\rm sh}=1.74v_{\rm A}$. The other parameters are the same as those in the previous run. In this example, the particle barely penetrates the shock region twice and gains energy twice. Then, its $v_{\parallel x}$ eventually becomes greater than $v_{\rm sh}$, and it goes ahead of the pulse. Figure 10 shows an example for a shock wave with propagation angle $\theta=64°$; the largest angle in the three examples. The propagation speed is $v_{\rm sh}=2.01v_{\rm A}$. Here, the particle was accelerated four times. The strong interaction had not been finished ($v_{\parallel x}$ had not exceeded $v_{\rm sh}$), when the simulation was terminated.

## IV. SUMMARY AND DISCUSSION

We have theoretically and numerically studied interactions of energetic ions with a shock wave propagating obliquely to a magnetic field. First, we analyzed motions of energetic ions that barely penetrate the shock region. The change in the magnetic field in an oblique shock wave can increase $p_\parallel$ at the moments when the energetic ions enter and go out of the shock region. In this process, the particle energy is not changed; hence $p_\perp$ decreases when $p_\parallel$ increases. On the other hand, while these particles are in the shock region, they can continuously gain energies from the transverse electric field. Next, we further investigated the interactions by using a one-dimensional, fully electromagnetic, relativistic particle simulation code with full ion and electron dynamics. It was found that some energetic ions, but not all, can move with a shock wave for long periods of time; during which the processes mentioned above can take place several times in the shock wave.

Even if the initial $v_{\parallel x}$, the $x$ component of the parallel velocity, is lower than the shock propagation speed $v_{\rm sh}$, it can be close to $v_{\rm sh}$ by the increase in $p_\parallel$ through the interaction with the magnetic field. Some of these particles can thus move with the shock wave and can be accelerated many times by the transverse electric field. After some periods of time, however, these particles have $v_{\parallel x}$ higher than $v_{\rm sh}$ and go away from the shock region to the upstream region.

Using the angle $\theta$ between the magnetic field and the direction of the wave propagation, we can rewrite the condition $v_{\parallel x}\sim v_{\rm sh}$ as

$$v_\parallel \cos\theta \sim v_{\rm sh}. \tag{33}$$

Here, we can roughly interpret the angle $\theta$ as the one in the

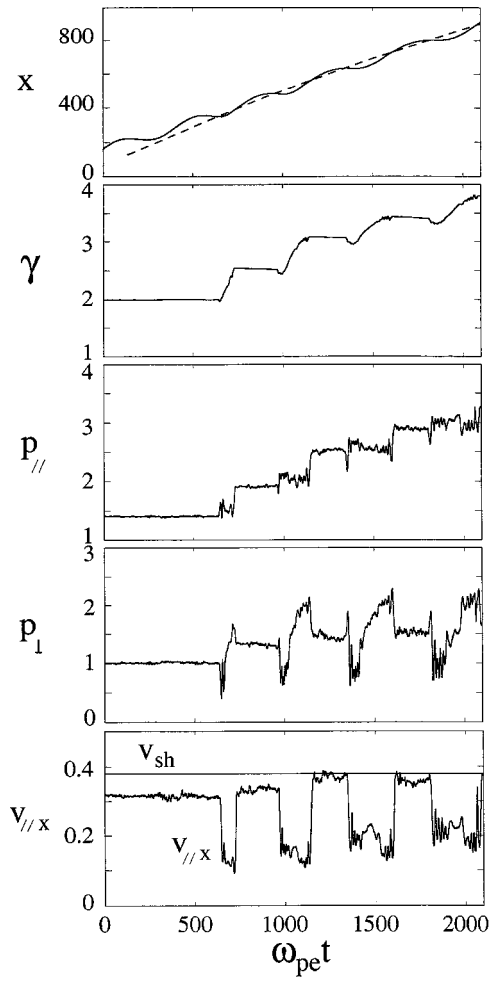


FIG. 10. Time variations of $x$, $\gamma$, $p_{\parallel}$, $p_{\perp}$, and $v_{\parallel x}$ of an energetic ion accelerated in an oblique shock wave with $\theta=64°$.

upstream region, even though, strictly speaking, $\theta$ depends on $x$. This equation tells us some important properties of this mechanism.

First, few thermal ions would satisfy this condition in a low beta plasma, where the Alfvén speed is much faster than the ion thermal speed. Hence, this mechanism can actually apply to energetic particles whose $v_{\parallel}$ are greater than the Alfvén speed. (It should also be noted that the theory in Sec. II was for energetic particles; the analysis was based on the assumption that the gyro-radius was much greater than the shock width.)

Second, unlimited acceleration could occur if

$$c\cos\theta \sim v_{\mathrm{sh}}. \tag{34}$$

In relativistic particles, $p_{\parallel}$ can be increased indefinitely. However, $v_{\parallel}$ is limited by the speed of light $c$. There is a possibility, therefore, that particle energy is increased repeatedly by this mechanism and, at the same time, the particle cannot escape from the shock wave ($v_{\parallel x}$ cannot exceed $v_{\mathrm{sh}}$).

In this connection, it is interesting to note that the energy $\gamma$ jumped twice in Fig. 9 where the angle was $\theta=45°$, while $\gamma$ jumped four times in Fig. 10 where $\theta=64°$; in the latter case the strong interaction was not finished yet when the simulation was terminated. At least, therefore, we can say that particles tend to need longer periods of time to have $v_{\parallel x}$ faster than $v_{\mathrm{sh}}$ if the value of $v_{\mathrm{sh}}/\cos\theta$ is closer to $c$.

In this paper we described a new acceleration phenomenon and its mechanism. As future work, it would be desirable to develop this study from statistical aspects. Also, it would be important to explore the acceleration under the condition (34). It is interesting to note that this condition coincides with the one for extremely strong electron acceleration in oblique shock waves.[18]

## ACKNOWLEDGMENTS

One of the authors (Y. O.) is grateful to Dr. Richard Sydora (University of Alberta) for stimulating discussions.

This work was supported in part by the National Science and Engineering Research Council of Canada, Contract No. NSERC-RGPIN205068, and by the Theoretical Physics Institute, University of Alberta.

[1] E. L. Chupp, H. Debrunner, E. Flückiger *et al.*, Astrophys. J. **318**, 913 (1987).
[2] K. Koyama, R. Petre, E. V. Gotthelf *et al.*, Nature (London) **378**, 255 (1995).
[3] T. Tanimori, Y. Hayami, S. Kamei *et al.*, Astrophys. J. Lett. **497**, L25 (1998).
[4] T. Tanimori, K. Sakurazawa, S. A. Dazeley *et al.*, Astrophys. J. Lett. **492**, L33 (1998).
[5] C. Joshi, C. E. Clayton, W. B. Mori, J. M. Dawson, and T. Katsouleas, Comments Plasma Phys. Control. Fusion **16**, 65 (1994).
[6] J. E. Gunn and J. P. Ostriker, Phys. Rev. Lett. **22**, 728 (1969).
[7] V. S. Beresinskii, S. V. Bulanov, V. A. Dogiel, V. L. Ginzburg, and V. S. Ptuskin, *Astrophysics of Cosmic Rays* (North-Holland, Amsterdam, 1990).
[8] D. Biskamp and H. Welter, Nucl. Fusion **12**, 663 (1972).
[9] M. M. Leory, D. K. Winske, C. C. Goodrich, C. S. Wu, and K. Papadopoulos, J. Geophys. Res. **87**, 5081 (1982).
[10] D. W. Forslund, K. B. Quest, J. U. Brackbill, and K. Lee, J. Geophys. Res. **89**, 2142 (1984).
[11] Y. Ohsawa, Phys. Fluids **28**, 2130 (1985).
[12] Y. Ohsawa, J. Phys. Soc. Jpn. **55**, 1047 (1986).
[13] B. Lembege and J. M. Dawson, Phys. Fluids B **1**, 1001 (1989).
[14] R. L. Tokar, S. P. Gary, and K. B. Quest, Phys. Fluids **30**, 2569 (1987).
[15] M. Toida and Y. Ohsawa, J. Phys. Soc. Jpn. **64**, 2038 (1995).
[16] M. Toida and Y. Ohsawa, Sol. Phys. **171**, 161 (1997).
[17] N. Bessho, K. Maruyama, and Y. Ohsawa, J. Phys. Soc. Jpn. **68**, 1 (1999).
[18] N. Bessho and Y. Ohsawa, Phys. Plasmas **6**, 3076 (1999).
[19] R. Z. Sagdeev and V. D. Shapiro, Zh. Eksp. Teor. Fiz. Pis'ma Red. **17**, 387 (1973) [Zh. Eksp. Teor. Fiz. Pis'ma Red. **17**, 279 (1973)].
[20] Y. Ohsawa, J. Phys. Soc. Jpn. **59**, 2782 (1990).
[21] M. A. Lee, V. D. Shapiro, and R. Z. Sagdeev, J. Geophys. Res. **101**, 4777 (1996).
[22] B. Rau and T. Tajima, Phys. Plasmas **5**, 3575 (1998).
[23] R. A. Mewaldt, R. S. Selesnick, J. R. Cummings, E. C. Stone, and T. T. von Rosenvinge, Astrophys. J. Lett. **466**, L43 (1996).
[24] K. Maruyama, N. Bessho, and Y. Ohsawa, Phys. Plasmas **5**, 3257 (1998).
[25] T. Masaki, N. Bessho, and Y. Ohsawa, Acceleration of energetic ions by oblique magnetosonic shock waves, to be published in J. Plasma Fusion Res.
[26] J. H. Adlam and J. E. Allen, Philos. Mag. Suppl. , 3 (448)1958.
[27] L. Davis, R. Lüst, and A. Schlüter, Z. Naturforsch. A **13**, 916 (1958).
[28] C. S. Gardner and G. K. Morikawa, Commun. Pure Appl. Math. **18**, 35 (1965).
[29] Y. Ohsawa, Phys. Fluids **29**, 2474 (1986).
[30] T. Kakutani, H. Ono, T. Taniuti, and C. C. Wei, J. Phys. Soc. Jpn. **24**, 1159 (1968).
[31] Y. Ohsawa, Phys. Fluids **29**, 1844 (1986).
[32] P. C. Liewer, A. T. Lin, J. M. Dawson, and M. Z. Caponi, Phys. Fluids **24**, 1364 (1981).
[33] Y. Ohsawa and J. M. Dawson, Phys. Fluids **27**, 1491 (1984).